

**Enhancement of nitrous oxide emissions in soil microbial consortia via copper competition
between proteobacterial methanotrophs and denitrifiers**

Jin Chang,^{a,b} Daehyun Daniel Kim,^a Jeremy D. Semrau,^b Juyong Lee,^a Hokwan Heo,^a Wenyu Gu,^{b,*}
Sukhwan Yoon^{a,#}

^aDepartment of Civil and Environmental Engineering, Korea Advanced Institute of Science and
Technology, Daejeon, 34141, Korea

^bDepartment of Civil and Environmental Engineering, University of Michigan, Ann Arbor, MI, 48109

Running Title: Methanotrophic influence on N₂O emissions

#Address correspondence to Sukhwan Yoon, syoon80@kaist.ac.kr.

***Present address:** Department of Civil & Environmental Engineering, Stanford University, Palo Alto
CA, 94305

Abstract

Unique means of copper scavenging have been identified in proteobacterial methanotrophs, particularly the use of methanobactin, a novel ribosomally synthesized post-translationally modified polypeptide that binds copper with very high affinity. The possibility that copper sequestration strategies of methanotrophs may interfere with copper uptake of denitrifiers *in situ* and thereby enhance N₂O emissions was examined using a suite of laboratory experiments performed with rice paddy microbial consortia. Addition of purified methanobactin from *Methylosinus trichosporium* OB3b to denitrifying rice paddy soil microbial consortia resulted in substantially increased N₂O production, with more pronounced responses observed for soils with lower copper content. The N₂O emission-enhancing effect of the soil's native *mbnA*-expressing *Methylocystaceae* methanotrophs on the native denitrifiers was then experimentally verified with a *Methylocystaceae*-dominant chemostat culture prepared from a rice paddy microbial consortium as the inoculum. Lastly, with microcosms amended with varying cell numbers of methanobactin-producing *Methylosinus trichosporium* OB3b before CH₄ enrichment, microbiomes with different ratios of methanobactin-producing *Methylocystaceae* to gammaproteobacterial methanotrophs incapable of methanobactin production were simulated. Significant enhancement of N₂O production from denitrification was evident in both *Methylocystaceae*-dominant and *Methylococcaceae*-dominant enrichments, albeit to a greater extent in the former, signifying the comparative potency of methanobactin-mediated copper sequestration while implying the presence of alternative copper abstraction mechanisms for *Methylococcaceae*. These observations support that copper-mediated methanotrophic enhancement of N₂O production from denitrification is plausible where methanotrophs and denitrifiers cohabit.

Importance

Proteobacterial methanotrophs, groups of microorganisms that utilize methane as source of energy and carbon, have been known to utilize unique mechanisms to scavenge copper, namely utilization of methanobactin, a polypeptide that binds copper with high affinity and specificity. Previously the possibility that copper sequestration by methanotrophs may lead to alteration of cuproenzyme-

mediated reactions in denitrifiers and consequently increase emission of potent greenhouse gas N₂O has been suggested in axenic and co-culture experiments. Here, a suite of experiments with rice paddy soil slurry cultures with complex microbial compositions were performed to corroborate that such copper-mediated interplay may actually take place in environments co-habited by diverse methanotrophs and denitrifiers. As spatial and temporal heterogeneity allow for spatial coexistence of methanotrophy (aerobic) and denitrification (anaerobic) in soils, the results from this study suggest that this previously unidentified mechanism of N₂O production may account for significant proportion of N₂O efflux from agricultural soils.

Introduction

Methane (CH₄) and nitrous oxide (N₂O) are the most influential greenhouse gases apart from CO₂, with estimated contributions of 16% and 6.2% to global greenhouse gas emissions over a 100-year-time frame (1). Biological sources and sinks significantly impact both atmospheric CH₄ and N₂O pools. That is, methanotrophs consume much (up to 100%) of CH₄ originating from methanogenesis, balancing the global CH₄ budget (2). Similarly, N₂O produced via microbially-mediated nitrification and denitrification is offset by N₂O reduction mediated by microbes capable of expressing and utilizing nitrous oxide reductases (NosZ) (3-5). Collectively, the relative abundance and activity of different microbial groups are critical in determining if any particular environment is a net source or sink of these potent greenhouse gases.

Methanotrophy has become a rather comprehensive term following recent discovery of extremophilic verrucomicrobial methanotrophs, nitrite-reducing anaerobic NC-10 methanotrophs, and archaeal anaerobic methanotrophs (6-9); however, except for certain specialized extreme habitats, “conventional” aerobic proteobacterial methanotrophs often dominate methane oxidation *in situ*, especially in terrestrial systems, e.g., oxic-anoxic interfaces of rice paddy soils and landfill cover soils, as observed in recent metagenomic analyses (10, 11). Proteobacterial methanotrophs are phylogenetically subdivided into gammaproteobacterial and alphaproteobacterial subgroups (12).

Both of these organismal groups utilize particulate and/or soluble methane monooxygenases (MMO) encoded by *pmo* and *mmo* operons, respectively, and these MMOs are currently known as the only enzymes capable of preferentially catalyzing the oxidation of CH₄ to CH₃OH (13). Of the two forms of MMOs, the particulate methane monooxygenase (pMMO) has been regarded as the prevalent form in most terrestrial environments, and the majority of proteobacterial methanotroph genomes sequenced to date contain only *pmo* operon(s) (14). The expression and activity of pMMO are strongly dependent on copper, although the exact role of copper in pMMO still remains unanswered (12, 15, 16).

Due to the dependency of pMMO activity on copper, pMMO-expressing methanotrophs have high demands for copper (17). Not surprisingly, methanotrophs have developed effective copper uptake mechanisms, presumably to cope with limited copper availability *in situ*. Some alphaproteobacterial methanotrophs of the *Methylocystaceae* family produce and excrete methanobactin, a modified peptide ~800-1300 Da in size that chelates copper with the highest affinity among known metal chelators (empirical copper-binding constants range between 10¹⁸-10⁵⁸ M⁻¹ depending on experimental protocol used) (18). Methanobactin has high specificity towards copper, and binding constants higher than 10⁹ M⁻¹ have been observed only for its complexation with Cu⁺, Cu²⁺ (reduced to Cu⁺ upon binding), Au³⁺, and Hg²⁺ (17). Copper-bound methanobactin is transported into the cell via a TonB-dependent transporter and presumably utilized for synthesis of a functional pMMO complex (19, 20). The genes encoding for the methanobactin polypeptide precursor (*mbnA*) and the enzymes involved in its post-translational modifications have been identified in many alphaproteobacterial methanotroph genomes (roughly half of >40 genomes currently available in the NCBI database), and methanobactin isolated from seven distinct strains of *Methylocystaceae* methanotrophs have been chemically characterized, suggesting that the capability to synthesize and utilize methanobactin is a wide-spread, but not universal, trait for *Methylocystaceae* methanotrophs (18, 21-24).

In CH₄-rich, copper-depleted environments, these copper acquisition mechanisms of methanotrophs may interfere with other biogeochemical reactions catalyzed by cuproenzymes. Several key enzymes involved in the biological nitrogen cycle including bacterial and archaeal ammonia monooxygenases (AMO), copper-dependent NO₂⁻ reductases (NirK), and N₂O reductases (NosZ) require copper ions for their activity (25-27). The impact on NosZ expression and activity would be particularly consequential from an environmental perspective, as NosZ-catalyzed N₂O reduction is the only identified biological or chemical N₂O sink in the environment (3, 28). Ammonia oxidation mediated by bacterial AMO retains its activity at copper-deficient incubation condition (i.e., nanomolar bioavailable Cu concentration), and NO₂⁻ reduction to NO in denitrifiers can be carried out by Cu-independent cytochrome *cd*₁ nitrite reductase (NirS); however, no copper-independent alternative pathway for N₂O reduction to N₂ has been identified to date (3, 29). In fact, methanobactin-mediated inhibition of NosZ activity was recently experimentally verified *in vitro* using simple, well-defined co-cultures of *M. trichosporium* OB3b and several denitrifier strains possessing *nosZ*, suggesting the possibility of increased N₂O emissions *in situ* where methanotrophs and denitrifiers co-exist (30). Oxic-anoxic interfaces and the vadose zones with fluctuating water content would provide settings in organic- and nitrogen-rich soils, where co-occurrence of obligately aerobic methanotrophy and obligately anaerobic denitrification is possible (31, 32). Whether such an N₂O-production mechanism is truly relevant in the field, however is not yet known, as neither methanobactin production nor its influence on denitrifiers has been observed in complex microbiomes such as agriculture soils.

As a follow-up to our previous study documenting the impact of methanobactin-producing methanotroph on denitrification and N₂O production in simple co-cultures, the current study investigated further the potential ecological relevance of this methanotroph-denitrifier interaction by introducing microbial complexity and competition into the picture. The susceptibility of soil's complex denitrifying consortia to methanobactin-mediated alteration was examined with (1) denitrifying enrichments amended with exogenous addition of methanobactin and (2) stimulation of native alphaproteobacterial methanotrophs of the *Methylocystaceae* family. Further, the consequence

of alphaproteobacterial methanotrophs-vs-gammaproteobacterial methanotrophs competition on denitrification and associated N₂O production was examined with soil slurry microcosms augmented with varying amounts of *M. trichosporium* OB3b before CH₄ enrichment.

Results

The effect of methanobactin from *M. trichosporium* OB3b on N₂O production in denitrifying soil enrichments

The effect of the methanobactin isolated from *M. trichosporium* OB3b (MB-OB3b) on N₂O production was examined with NO₃⁻-reducing enrichments of five rice paddy soils with varying copper content (Fig. 1; Supplementary Table S1). Without added MB-OB3b, the amount of accumulated N₂O-N did not exceed 0.2% of ~250 μmoles NO₃⁻ initially added to the reaction vessels at any time in any of the enrichment cultures despite four out of five soil samples being slightly acidic with 5.8<pH<6.3 (Fig. 1A-E). In contrast, substantial N₂O accumulation was observed in soil slurry cultures amended with 10 μM MB-OB3b, with the exception of soil with the highest copper content (Fig. 1F-J). Permanent N₂O accumulation was observed in the enrichments prepared with the soils with the lowest copper content (A: 1.14±0.06 mg Cu/kg dry wt; B: 1.50±0.02 mg Cu/kg dry wt), with 138±2 and 102±11 μmoles N₂O-N produced from denitrification of 257±29 and 275±5 μmoles NO₃⁻, respectively. Although the non-stoichiometric N₂O production suggested partial N₂O reduction activity, no further N₂O reduction was observed for at least 24 h after completion of denitrification in either enrichment. Inhibition of NO₂⁻ reduction was also evident in the Soil B enrichment (Fig. 1G). Permanent N₂O accumulation and delayed NO₂⁻ reduction was observed also with the enrichment prepared with Soil C that had a higher copper content (2.78±0.28 mg Cu/kg dry wt; Fig. 1H). The enrichments prepared with soils with the highest copper contents (D: 5.73±0.38 mg Cu/kg dry wt; E: 8.05±0.34 mg Cu/kg dry wt) did not permanently accumulate N₂O even with 10 μM methanobactin added; however, the maximum amount of transiently accumulated N₂O was significantly higher (*p*<0.05) with methanobactin than without. No significant NO₃⁻ or NO₂⁻ reduction was observed in any of the sterilized controls, and N₂O production over 120 hours of abiotic incubation yielded <1.0

$\mu\text{moles N}_2\text{O-N}$, precluding the possibility that abiotic N_2O production contributed significantly to N_2O produced in the NO_3^- -reducing soil enrichments (data not shown). These results demonstrated that methanobactin can inhibit N_2O and/or NO_2^- reduction in complex microbial consortia, but the effect may vary depending on soil properties.

Denitrification and N_2O accumulation in a soil microbial consortium enriched with indigenous *Methylocystaceae* methanotrophs

To observe whether indigenous soil methanotrophs are capable of altering soil denitrification and enhancing N_2O production with methanobactin as the mediator, denitrification was observed with *Methylocystaceae*-dominant quasi-steady state culture extracted from a chemostat (Fig. 2, Supplementary Table S2). The copy number of eubacterial 16S rRNA genes in the quasi-steady state reactor culture was $1.52 \pm 0.02 \times 10^6$ copies mL^{-1} . Alphaproteobacterial methanotrophs of the *Methylocystaceae* family were the dominant bacterial population, with 78 % of the 16S rRNA reads assigned to OTUs affiliated with this taxon, while the OTUs assigned to the gammaproteobacterial methanotrophs (the *Methylococcaceae* family) constituted a minority group with 1.5 % relative abundance. Non-methanotrophic taxa identified in the reactor culture included *Chitinophagaceae* (7.3%), *Pseudomonadaceae* (1.4%), and *Mycobacteriaceae* (1.3%). The most abundant *nirK* and *nosZ* recovered from the metagenome of the chemostat culture were most closely affiliated in terms of translated amino acid sequences to *Methylocystis* sp. Rockwell (69 % of recovered *nirK*) and *Methylocystis* sp. SC2 (93 % of recovered *nosZ*), both of which are the only *nirK* and *nosZ* found in sequenced alphaproteobacterial methanotroph genomes (Supplementary Table S3). The other *nirK* genes recovered with >1% relative abundance (among the recovered *nirK* sequences) included those most closely affiliated to the genera *Mesorhizobium* (16 %), *Bauldia* (3.5%), *Panacibacter* (3.1%), *Pseudomonas* (1.8%), and *Hypomicrobium* (1.4%). The most abundant non-methanotrophic *nosZ* genes included those affiliated to the genera *Flavobacterium* (3.4%; clade II) and *Pseudomonadas* (2.5%; clade I). The coverage of *nirS* genes were substantially lower than those of *nirK* (2.1×10^{-3} *nirS/recA* as compared to 0.133 total *nirK/recA* and 4.2×10^{-2} non-*Methylocystis nirK/recA*). The

recovered *nirS* genes included those affiliated to the genera *Bradyrhizobium* (29.0% of recovered *nirS*), *Zoogloea* (41.0%), and *Acidovorax* (31.9%).

The sole unique *mbnA* sequence assembled from the shotgun metagenome reads exhibited high similarity to *mbnA* sequences of organisms affiliated to the *Methylocystis* genus (Supplementary Fig. S1). The qPCR quantification targeting the *Methylocystaceae* *mbnA* genes estimated $8.1 \pm 1.8 \times 10^4$ copies mL⁻¹, which translated to an *mbnA*-to-16S rRNA ratio of 0.054. Further, the *mbnA* transcript-to-gene ratio was 19.5 ± 4.9 as determined using RT-qPCR, indicating that the *mbnA* gene was actively transcribed during quasi-steady state operation of the reactor.

Reduction of NO₃⁻ was observed immediately after addition of the denitrifying inoculum to the degassed CH₄-enriched culture extracted from the chemostat and was unaffected by Cu²⁺ amendment (Fig. 2B). Repression of NO₂⁻ reduction was apparent in the culture without Cu²⁺ amendment, as no significant decrease in NO₂⁻ concentration was observed for ~20 hours after maximum NO₂⁻ accumulation was observed (414 ± 29 μmoles NO₂ at t=18.5 h). Eventual reduction of NO₂⁻ led to transient accumulation of N₂O, and the maximum amount of N₂O observed before it was presumably reduced to N₂ was 155 ± 25 μmoles N₂O-N (~32% of added NO₃⁻-N). Such apparent partial repression of NO₂⁻ and N₂O reduction was absent in the samples amended with 2 μM Cu²⁺. NO₂⁻ reduction progressed without any apparent lag, and the amount of N₂O in the vessel did not increase higher than 0.09 ± 0.01 μmoles N₂O-N before it was consumed. These observations suggest that alteration of copper availability by methanobactin-producing *Methylocystaceae* methanotrophs had substantial effect on denitrification and N₂O reduction in the broader microbial community.

Effects of altered community compositions of methanotrophic enrichments on denitrification and N₂O production upon transition to anoxia

Methanotroph-enriched microbiomes with different ratios of methanobactin-producing *Methylocystaceae* to gammaproteobacterial methanotrophs were mimicked in soil slurry microcosms

by adding varying amounts of *M. trichosporium* OB3b precultures to rice paddy soil slurries before batch enrichment with 20% v/v CH₄ (Fig. 3). The 16S rRNA gene copy number of *Methylococcaceae* methanotrophs in the soil sample was estimated to be $6.5 \pm 1.2 \times 10^6$ copies g wet wt soil⁻¹ from their relative abundance (0.41%) and the total bacterial 16S rRNA copy number ($1.6 \pm 0.3 \times 10^9$ bacterial 16S rRNA copies g wet wt soil⁻¹). *Methylosinus trichosporium* OB3b *pmoA* copy numbers in the CH₄-enriched slurries were 0, $1.2 \pm 0.2 \times 10^6$, and $3.3 \pm 0.7 \times 10^8$ per mL in the cultures that had been augmented with *M. trichosporium* OB3b *pmoA* copy numbers in quantities matching 0, 1, and 10 times the estimated 16S rRNA gene copy numbers affiliated to *Methylococcaceae* methanotrophs (referred to as *mtri0*, *mtri1*, and *mtri10*, respectively). The 16S rRNA amplicon sequencing of the same samples estimated the relative abundances of *Methylocystaceae* methanotrophs to be 0.15, 0.35 and 13.0%, respectively (Supplementary Table S4). The relative abundances of *Methylococcaceae* methanotrophs were 39, 7.7, and 0%, respectively, in the same samples.

In the *mtri0* culture, the maximum amount of accumulated N₂O was 49.6 ± 14.5 μmoles N₂O-N and the duration of N₂O accumulation was shorter than 10 h (Fig. 3). The maximum observed N₂O accumulation (78.2 ± 16.4 μmoles N₂O-N at t=50 h) was significantly higher ($p < 0.05$) and the duration of N₂O accumulation substantially longer (68.5 h) in the *mtri10* cultures, in which *Methylocystaceae* methanotrophs outnumbered *Methylococcaceae* methanotrophs. The decrease in the amount of NO₃⁻ observed during active CH₄ oxidation (t < 10.5 h) was presumably due to assimilation, as denitrification was unlikely to occur before O₂ depletion. Thus, N₂O accumulation resulting from dissimilatory reduction of NO₃⁻ between 10.5 and 94 h was near stoichiometric, albeit transient, in the *mtri10* cultures. In the *mtri1* cultures, the maximum amounts of accumulated N₂O were significantly lower ($p < 0.05$) than either the *mtri0* and *mtri10* cultures, in line with the substantially lower methanotroph population.

In the negative control experiment performed with the $\Delta mbnAN$ mutant strain added to the soil suspension in place of the wildtype *M. trichosporium* OB3b (referred to as *mtri10n*), the maximum

amount of N₂O accumulated in the vessel was limited to 0.27±0.09 μmoles N₂O-N despite the *Methylocystaceae* dominance of the methanotrophic population, as indicated by the high *M. trichosporium* OB3b *pmoA* copy numbers (1.2±0.7×10⁸ per mL) and the low *Methylococcaceae*-to-*Methylocystaceae* population ratio (0.21) in the *mtri10n* culture (Fig. 3). The results of this control experiment confirmed that the enhanced N₂O accumulation of the *Methylocystaceae*-dominant enrichment was due to copper sequestration by methanobactin produced by *M. trichosporium* OB3b. Also notable was the obvious dissimilarity observed in the microbial community composition between the enrichments with the wildtype strain OB3b and $\Delta mbnAN$ mutant strain (Fig. 3, Supplementary Table S4). The additional set of control experiment performed with 2.0 μM CuCl₂ added to the soil-only, thus *Methylococcaceae*-dominant, samples (referred to as *mtri0c*), suggested that the instantaneous N₂O accumulation observed in the *Methylococcaceae*-dominant culture could also be explained as the effect of Cu²⁺ sequestration by the methanotrophic population. The maximum N₂O production (3.75±1.25 μmoles N₂O-N at t=106 h) was ~13 times lower with Cu²⁺ added than without despite the abundance of *Methylococcaceae* family of methanotrophs (48.5% of 3.5±0.2×10⁸ eubacterial 16S rRNA copies mL⁻¹).

Discussion

Copper deficiency has been suggested as a potential cause for N₂O emission from denitrification taking place in terrestrial and aquatic environments (33-35). In a previous study, Chang et al. demonstrated, using simplified pure-culture and co-culture experiments, that MB-OB3b lowered copper availability of the medium such that N₂O reduction was substantially repressed in denitrifiers (30). Whether methanobactin-mediated N₂O emission enhancement is relevant to actual soil environments with much more intricate microbiome complexity remained to be resolved, however. The results of the experiments in this study, although performed under well-controlled laboratory conditions, showed that methanobactin-enhanced N₂O emissions may actually occur in soil environments with complex microbiomes. Methanobactin addition exerted significant influence on denitrification carried out by soils' indigenous microbial consortia, demonstrating that diverse

denitrifying community was still susceptible to methanobactin-mediated copper deprivation. Further, the N₂O emission enhancement observed with the *Methylocystaceae* methanotroph-enriched reactor culture provided an unprecedented experimental evidence of indigenous alphaproteobacterial methanotrophs influencing N₂O emission from denitrifiers. Observation of substantial *mhnA* transcription and the absence of this N₂O emission enhancement effect in the copper-amended sample supported that methanobactin produced by the indigenous *Methylocystaceae* methanotrophs was likely the cause of the increased N₂O production from denitrification. Additionally, the increased N₂O production observed in soil enrichments with broadly varying *Methylocystaceae*-to-*Methylococcaceae* ratios suggested that methanotrophic population composition *in situ* may be a major determinant of the copper-mediated N₂O emission enhancement, while also suggesting existence of an additional mechanism via which methanotrophs affect N₂O reduction in denitrifiers.

Evidence of the effect of methanobactin on the soil microbial consortia apart from N₂O emission enhancement could also be discerned. Delays in NO₂⁻ reduction during the progression of denitrification were observed in some, but not all, of denitrifying enrichments incubated in the presence of OB3b-MB capable of producing methanobactin. At least two distinct forms of nitrite reductases are known to mediate NO₂⁻-to-NO reduction in denitrifiers: the copper-dependent nitrite reductase NirK and copper-independent cytochrome *cd*₁ nitrite reductase NirS (36). In the previous investigation by Chang et al., indeed, NO₂⁻ reduction by NirK-utilizing *Shewanella loihica*, but not NirS-utilizing denitrifiers, was affected by methanobactin-mediated Cu deprivation (30). The environmental conditions that select for enrichment of either NirK- or NirS-utilizing organisms remain unclear, and abundances of *nirS*- or *nirK*-possessing organisms vary in rice paddy soils (37). Possibly, the relative abundances and activities of the NirK- and NirS-utilizing denitrifiers may have varied in the denitrifying consortia prepared with soils A-E, explaining the non-uniform responses of the denitrifiers in the consortia to copper deprivation. That copper addition expedited NO₂⁻ reduction in anoxic incubation of *nirK*-dominant chemostat culture was also in support of this hypothesis.

The shotgun metagenome analyses of the methanotrophic chemostat culture identified the organisms affiliated to the *Methylocystaceae* family as the dominant *nirK*-possessing organisms. Further, the *nosZ* gene affiliated to *Methylocystis* sp. SC2 was the dominant *nosZ* gene in the chemostat culture (38). These observations are certainly interesting, as the only *Methylocystaceae nirK* and *nosZ* sequences available in the database are the *nirK* gene found in the genome of *Methylocystis* sp. Rockwell and the *nosZ* gene found in a plasmid of *Methylocystis* sp. SC2 (38, 39). Both genes were unique, in a sense that they both shared <75% translated amino acid sequence identity with any other NirK or NosZ sequences in the NCBI database, and no previous study has reported recovery of these *Methylocystaceae nirK* and *nosZ* sequences in metagenome/metatranscriptome analyses. Despite the potential significance of the discovery, the possibility that the *Methylocystaceae* methanotrophs harboring these genes might have significantly affected NO₂⁻ reduction and N₂O production in the anoxic batch incubations was highly unlikely. Both *Methylocystis* sp. Rockwell and *Methylocystis* sp. SC2 have been confirmed of their inability to grow anaerobically, and neither strain has been confirmed of capability to reduce NO₂⁻ or N₂O utilizing NirK or NosZ, respectively (38, 39). Therefore, although the collected data are insufficient to completely rule out the possibility that these *Methylocystaceae* populations significantly contributed to denitrification and N₂O production and consumption, it is more plausible that the N₂O dynamics in the anoxic cultures were largely determined by non-methanotrophic facultatively anaerobic organisms carrying *nirK*, *nirS*, and/or *nosZ* genes.

In this metagenome analysis, many of the non-methanotrophic organisms putatively harboring *nirK* or *nirS* and those putatively harboring *nosZ* belonged to different taxa, suggesting that N₂O production and N₂O consumption were carried out by distinct organismal groups in the anoxic batch experiments performed with this chemostat culture. For example, the dominant non-*Methylocystaceae nirK* and *nosZ* recovered from the chemostat metagenome were those affiliated to *Rhizobiales* and *Bacteroidetes*, respectively, and only *nirK* and *nosZ* affiliated to *Pseudomonaceae* were recovered with similar coverage. These observations suggest that the alteration of copper availability brought

about by methanobactin-producing methanotrophs may influence N₂O emissions from denitrification occurring in modular manner, which may be the more likely case in complex environmental microbiomes (40, 41).

The distinctive contrast between the microbial compositions between the *mtri10* and *mtri10n* enrichments implied that methanobactin had pronounced impact on the overall microbial community. The microbial community formed from enrichment on CH₄ and acetate after augmentation with the wildtype strain OB3b (*mtri10*) carried distinctively large proportion of *Moraxellaceae* (44.7%). Such abundance of *Moraxellaceae* was not observed in the enrichment with augmented $\Delta mbnAN$ mutant cells (*mtri10n*), suggesting that this enrichment of *Moraxellaceae* was due to the presence of methanobactin produced by *M. trichosporium* OB3b. The most probable explanations are selective bactericidal property and/or reduced copper bioavailability to competing organisms with high demands for copper (18, 22). The relative abundance of other phylogenetic groups including *Methylophilaceae* and *Flavobacteriaceae* also varied substantially across the treatments. Unlike the case for *Moraxellaceae*, however, the experimental evidences were not sufficient to attribute these alterations to the effect of methanobactin.

The observed N₂O emission enhancement in methanotroph-enriched cultures dominated by the *Methylococcaceae* family, i.e., the *mtri0* enrichment, was unanticipated, as none of the sequenced genomes of the methanotrophs belonging to this phylogenetic group has been reported to produce methanobactin encoded by *mbnA* (18). What is evident from the experimental results, however, is that copper competition was central to N₂O production in these enrichments, as copper amendment removed the N₂O-accumulating phenotype. Indications that *Methylophilum album* BG8 and *Methylococcus capsulatus* Bath may utilize methanobactin-like copper chelators had been previously reported (42, 43). These *Methylococcaceae* strains tested positive on the Cu-CAS (chromo azurol S) plate assays, and the putative methanobactin-like compound of ~1000 Da in size isolated from the spent medium of *M. capsulatus* Bath bound Cu with 1:1 stoichiometry; however, the genomic basis

for synthesis of these compounds in *Methylococcaceae* methanotrophs has not yet been elucidated. Another copper uptake mechanism involving copper-binding periplasmic membrane proteins MopE and CorA have been identified in *M. capsulatus* Bath and *M. album* BG8, respectively (44, 45). The estimated binding constants of these putative copper chelators are tens of orders of magnitudes lower than those reported for methanobactin from *Methylocystaceae* methanotrophs; however, if present at large concentrations, the copper chelators may still exert significant impact on the Cu availability. Which, if any, of these mechanisms was responsible for copper withholding from denitrifiers and N₂O reducers in the *Methylococcaceae*-dominant enrichments cannot be determined with the current data and warrants future investigation.

One of the most prominent characteristics of soil environments is their spatial and temporal heterogeneity, both in terms of physico-chemical makeup and microbial composition (46, 47). In CH₄-enriched soil environments such as rice paddy and landfill soils, proteobacterial methanotrophs are often reported to be abundant, with *pmoA* copy numbers ranging between 10⁷ and 10¹⁰ gene copies g dry soil⁻¹ (48-50). These numbers are of the same magnitude as the methanotrophic populations in the enrichment cultures observed to induce N₂O production from the cohabiting denitrifying population in the laboratory experiments performed here. Methanotroph population density at local microsites may even be higher, especially at the oxic-anoxic interfaces, where CH₄ and O₂, the essential substrates of proteobacterial methanotrophs, are both available (49). Thus, it would not be surprising to find local concentrations of methanobactin-producing *Methylocystaceae* methanotroph communities in microniches within the soil sufficiently dense as to cause copper deficiency to cohabiting NosZ-utilizing N₂O reducers. At microscopic scale, temporal oxic-to-anoxic shifts or *vice versa* would constantly occur at the oxic-anoxic interfaces, allowing for spatial co-existence of O₂-dependent CH₄ oxidation and O₂-inhibited denitrification (32). The substrates of denitrification, NO₃⁻ and NO₂⁻, may be transported from oxic surface soils or supplied via oxidation of organic N or NH₄⁺ *in situ* at the oxic-anoxic interface with intermittently available O₂ (31). Periodic oxic-anoxic transitions may also take place in the vicinity of the water table in upland soils, as precipitation and

drying cause fluctuations in the elevation of the water table (51). In such settings, aerobic microbial processes of nitrification and methanotrophy and anaerobic microbial processes of denitrification and methanogenesis may alternate at a larger scale. Snapshot-views of physico-chemical and biological states of soils may cast doubt on the likelihood of the methanotroph-enhanced N₂O emissions occurring in actual soil environments; however, with these spatial and temporal shifts in consideration, the suggested mechanism is plausible in any terrestrial environment with high organic and nitrogen content. Thus, in approximating greenhouse gas budgets from environments such as rice paddy soils, landfill cover soils, wetland soils, and upland agricultural soils, N₂O arising from the copper-mediated interaction between methanotrophs and N₂O reducers need to be considered for development of a more accurate prediction model for N₂O emissions.

Methods and materials

Soil sampling and characterization

Soil samples were collected from an experimental rice paddy located at Gyeonggido Agricultural Research & Extension Services in Hwaseong, Korea (37°13'21"N, 127°02'35"E) in August 2017 and four rice paddies near Daejeon, Korea (36°22'41"N, 127°19'50"E) in December 2018 (Supplementary Table S1). Samples were collected from the top layer of soil (0-20 cm below the overlying water). After removing plant material, soil samples were stored in sterilized jars, which were then filled to the brim with rice paddy water. The samples were immediately transported to the laboratory in a cooler filled with ice and stored at 4 °C until use. A small portion (~50 g) of each collected soil was stored at -80 °C for DNA analyses.

The physicochemical characteristics of these soil samples were analyzed directly after sampling. The soil pH was measured by suspending 1 g wet weight soil in 5 mL Milli-Q water. Total nitrogen and carbon content of air-dried soil samples were analyzed with a Flash EA 1112 Elemental Analyzer (Thermo Fisher Scientific, Waltham, MA). For measurements of NH₄⁺, NO₃⁻, and NO₂⁻ content in soil samples, 1 g air-dried soil was suspended in 5 mL 2 M KCl solution and shaken at 200 rpm for an

hour. After settling the suspension for 10 min, the supernatant was passed through a 0.2 μM membrane filter (Advantec MFS Inc., Tokyo, Japan). The filtrate was analyzed using colorimetric quantification methods. The total copper content of soil samples was measured with an Agilent ICP-MS 7700S inductively coupled plasma mass spectrometer (Santa Clara, CA) after pretreatment with boiling aqua regia (52).

Media and culture conditions

Unless otherwise mentioned, modified nitrate mineral salts (NMS) medium was used for enrichment of methanotrophs in soil microbial consortia and incubation of axenic cultures of the wildtype and $\Delta mbnAN$ mutant strains of *M. trichosporium* OB3b (53). The medium contained per liter, 1 g $\text{MgSO}_4 \cdot 7\text{H}_2\text{O}$ (4.06 mM), 0.5 g KNO_3 (4.95 mM), 0.2 g $\text{CaCl}_2 \cdot 2\text{H}_2\text{O}$ (1.36 mM), 0.1 mL of 3.8% (w/v) Fe-EDTA solution (Sigma-Aldrich, St. Louis, MO), 0.5 mL of 0.02% (w/v) $\text{Na}_2\text{MoO}_4 \cdot 2\text{H}_2\text{O}$ solution, and 0.1 mL of the 10,000X trace element stock solution (Supplementary Table S5). All glassware used in this study was equilibrated in a 5 N HNO_3 acid bath overnight before use to reduce background contamination of copper to $<0.01 \mu\text{M}$ in media. Forty-milliliter aliquots of the medium was distributed into 250-mL serum bottles and the bottles were sealed with butyl-rubber stoppers (Geo-Microbial Technologies, Inc., Ochelata, OK, US) and aluminum caps. After autoclaving, the media were amended with 0.2 mL of 200X Wolin vitamin stock solution (Supplementary Table S6) and 500 mM pH 7.0 $\text{KH}_2\text{PO}_4/\text{Na}_2\text{HPO}_4$ solution was added to a final concentration of 5 mM (54). High-purity CH_4 (>99.95 %; Deokyang Co., Ulsan, Korea) replaced 20% of the headspace air. After inoculation, culture bottles were incubated in dark at 30 °C with shaking at 140 rpm.

Analytical procedures

Headspace CH_4 concentrations were measured using a GCMS-QP2020 gas chromatograph-mass spectrometer (Shimadzu Cooperation, Kyoto, Japan) equipped with a SH-RtTM-Q-BOND column (30 m length \times 0.32 mm inner diameter, 10 μm film thickness). The injector and oven temperatures were set to 150 °C and 100 °C, respectively, and helium was used as the carrier gas. Headspace N_2O

concentrations were measured with a HP 6890 Series gas chromatograph equipped with a HP-PLOT/Q column and an electron capture detector (Agilent, Palo Alto, CA, US). The injector, oven, and detector temperatures were set to 200, 85, and 250 °C, respectively. For each CH₄ or N₂O measurement, 50 µL or 100 µL of gas sampled using a Hamilton 1700-series gas-tight syringe (Reno, NV) was manually injected into the gas chromatographs. The dissolved N₂O concentrations were calculated from the headspace concentrations using the dimensionless Henry's law constant of 1.92 at 30°C (55, 56). The dissolved concentrations of NO₃⁻ and NO₂⁻ were determined colorimetrically using the Griess reaction (57). As the assay measures NO₂⁻, vanadium chloride (VCl₃) was used to reduce NO₃⁻ to NO₂⁻. The concentration of NH₄⁺ was measured using the salicylate method (58).

The total bacterial population was quantified using TaqMan-based quantitative polymerase chain reactions (qPCR) targeting eubacterial 16S rRNA gene (1055f: 5'-ATGGCTGTCGTCAGCT-3'; 1392r: 5'-ACGGGCGGTGTGTAC-3'; and Bac1115_probe: 5'-CAACGAGCGCAACCC-3')(59). The primers and probe set exclusively targeting the *pmoA* gene (encoding for the β subunit of particulate methane monooxygenase) of *M. trichosporium* OB3b (OB3b_pmoAf: 5'-CGCTCGACATGCGGATAT-3'; OB3b_pmoAr: 5'-TTTCCCGATCAGCCTGGT-3'; and OB3b_pmoA_probe: 5'-AGCCACAGCGCCGGAACCA-3') was designed *de novo* using Geneious v9.1.7 software (Biomatters Ltd., Auckland, New Zealand) and used for quantification of *M. trichosporium* OB3b cells. qPCR assays were performed with a QuantStudio™ 3 Real-Time PCR System (Thermo Fisher Scientific). The calibration curves for the targeted genes were constructed using serial dilutions of PCR2.1™ vectors (Thermo Fisher Scientific) carrying the target fragments. For each qPCR quantification, three biological replicates were processed separately. The complete list of the primers and probes used in this study are provided in Table 1.

Monitoring of denitrification and N₂O production in rice paddy soil suspensions amended with methanobactin from *M. trichosporium* OB3b

Methanobactin was isolated from *Methylosinus trichosporium* OB3b cultures and purified as previously described (60). The effects of MB-OB3b on N₂O emissions were examined with suspensions of five rice-paddy soils (soil A-E) with varying copper content. Each soil suspension was prepared by suspending 1 g of air-dried rice paddy soil into 50 mL Milli-Q water in 160-mL serum bottles and the headspace was replaced with N₂ gas after sealing. Methanobactin stock solution was prepared by dissolving 10 μmoles (11.5 mg) freeze-dried methanobactin in 10 mL Milli-Q water. The stock solution was equilibrated in an anaerobic chamber filled with 95% N₂ and 5% H₂ (Coy Laboratory Products Inc., Grass Lake, MI) for one hour to remove dissolved O₂, and 0.5 mL of the solution was added to the soil suspensions. Potassium nitrate and sodium acetate were then added to final concentrations of 5 mM and 10 mM, respectively. Soil suspensions were incubated with shaking at 140 rpm at 30°C. The headspace N₂O concentration and the dissolved concentrations of NO₃⁻ and NO₂⁻ were monitored until depletion of NO₃⁻ and NO₂⁻. The dissolved concentrations of NH₄⁺ were also monitored to ensure absence of significant dissimilatory nitrate reduction to ammonium (DNRA) activity. Negative controls were prepared identically, but without methanobactin amendment. Abiotic control experiments with sterilized soils with and without methanobactin amendment were performed with 5 mM NO₃⁻ or NO₂⁻ added, to confirm that abiotic contribution to N₂O production was minimal.

Monitoring of denitrification and N₂O production in subcultures extracted from a quasi-steady state chemostat culture of *Methylocystaceae*-dominated soil methanotrophs

A continuous methanotrophic enrichment culture was prepared with Soil E. The inoculum was generated by suspending 1 g (wet wt) soil in 50 mL NMS medium in a sealed 160-mL serum vial with air headspace. The vials were fed twice with 41 μmoles CH₄, yielding a headspace concentration of ~0.5% v/v upon each injection. After the initial batch cultivation, 20 mL of the enrichment was transferred to 5 L NMS medium in a 6-L fermenter controlled with a BioFlo[®] 120 Bioprocess Control Station (Eppendorf, Hamburg, Germany). Gas stream carrying a relatively low CH₄ concentration (0.5% v/v in air) was fed continuously at a rate of 145 mL min⁻¹ through a gas diffuser to stimulate growth of *Methylocystaceae* methanotrophs, as previous fed-batch and chemostat incubation of rice

paddy soils with a continuous supply of 20% v/v CH₄ resulted in domination by gammaproteobacterial methanotrophs (61). The reactor culture was maintained in the dark at pH 6.8 and 30 °C with agitation at 500 rpm. After the initial fed-batch operation, the reactor culture was transitioned to continuous operation with the dilution rate set to 0.014 h⁻¹. After quasi-steady state was attained, as indicated by constant effluent cell density and CH₄ concentration, 1.0-mL aliquots were collected and the pellets were stored at -20 °C for analyses of the microbial community composition and denitrification functional genes and qPCR quantification of *mbnA* and 16S rRNA genes. Additionally, 0.4-mL aliquots were treated with RNeasy Protect Bacteria Reagent (Qiagen, Hilden, Germany) and stored at -80 °C for reverse transcription qPCR (RT-qPCR) analyses of *mbnA* expression.

Triplicate anoxic batch cultures were prepared by distributing 50 mL culture harvested from the running quasi-steady state reactor to 160-mL serum bottles and flushing the headspace with N₂ gas. A denitrifying enrichment was prepared separately by incubating 1 g (wet wt) of Soil E in 100-mL anoxic NMS medium amended with 10 mM sodium acetate. One milliliter of this denitrifier inoculum was added to the methanotroph enrichments, to which 20 mM sodium acetate was added as the electron donor for denitrification. The cultures were amended with or without 2 μM CuCl₂ and the culture vessels were incubated in the dark with shaking at 140 rpm at 30 °C and the changes to the amounts of NO₃⁻, NO₂⁻, and N₂O-N in the vessels were monitored until no further change was observed.

Denitrification and N₂O production in soil enrichments with altered methanotrophic population composition

Varying amounts of pre-incubated *M. trichosporium* OB3b cells were added to rice paddy soil slurry microcosms before enrichment with CH₄, to artificially vary the proportion of the methanobactin-producing subgroup among the total methanotroph population. The total indigenous gammaproteobacterial methanotroph population in the soil suspension was approximated by

multiplying the total eubacterial 16S rRNA copy number per mL suspension (as determined with qPCR) by the proportion of the 16S rRNA gene sequences affiliated to gammaproteobacterial methanotrophs (all affiliated to the *Methylococcaceae* family) in soil “B” (as computed from the MiSeq amplicon sequencing data, Supplementary Table S7). The number of *M. trichosporium* OB3b cells in the precultures were estimated with the TaqMan qPCR targeting the duplicate *pmoA* genes of the strain. The *M. trichosporium* OB3b preculture was used to prepare soil suspensions with augmented *Methylocystaceae* population. The ratios of *M. trichosporium* OB3b *pmoA* copy numbers to the estimated 16S rRNA gene copy numbers of the *Methylococcaceae* methanotrophs were set to 1 and 10 in the 40 mL suspensions. It should be stressed that these ratios cannot be directly translated to cell number ratios, as the numbers of 16S rRNA genes in the completed genomes of gammaproteobacterial methanotrophs deposited in NCBI GenBank database vary between one and four. Soil suspensions without *M. trichosporium* OB3b augmentation was also prepared. As a negative control, the $\Delta mbnAN$ mutant strain of *M. trichosporium* OB3b was added in place of the wildtype strain OB3b (62). A copper-replete control was also prepared for the experimental condition with no *M. trichosporium* OB3b augmentation by amending a subset of cultures with 2 μM CuCl_2 .

The soil suspensions were prepared by adding 0.1 g wet wt of the soil to the autoclaved modified NMS medium bottles prepared as described above (40 mL NMS medium in 250-mL serum bottles). After sealing the bottles and adding *M. trichosporium* OB3b or $\Delta mbnAN$ mutant preculture or CuCl_2 to the calculated target concentrations, 20% of the headspace was replaced with CH_4 and sodium acetate was added to a final concentration of 5.0 mM. When the headspace CH_4 concentration decreased to 10%, the headspace was replenished with an 80:20 mixture of air and CH_4 , and the cultures were amended with 200 μmoles NO_3^- and 400 μmoles sodium acetate. At each sampling time point, the headspace N_2O concentration was measured and 0.5 mL of the culture collected from each bottle for determination of NO_3^- , NO_2^- , and NH_4^+ concentrations. The cell pellets collected immediately after CH_4 concentration dropped to ~10% were subjected to qPCR targeting strain OB3b

pmoA genes and eubacterial 16S rRNA genes. The 16S rRNA amplicon sequences of the pellets were also analyzed.

Microbial community composition analyses and prediction of genomic potentials for denitrification reactions from 16S rRNA amplicon sequences

Genomic DNA was extracted with DNeasy PowerSoil Kit (Qiagen, Hilden, Germany). The V6-V8 region of the 16S rRNA gene amplified with the universal primers 926F (5'-AAACTYAAAKGAATTGRCGG - 3')/1392R (5'-ACGGGCGGTGTGTRC-3') was sequenced at Macrogen Inc. (Seoul, Korea) using a MiSeq sequencing platform (Illumina, San Diego, CA)(63). The raw sequence data were processed using the QIIME pipeline v1.9.1 with the parameters set to default values (64). After demultiplexing and quality trimming, the filtered sequences were clustered into operational taxonomic units (OTUs) using USEARCH algorithm, and the OTUs were assigned taxonomic classification using the RDP classifier against the Silva SSU database release 132. The raw sequences were deposited to the NCBI SRA database (SRX8210313, SRX8209287-8209292).

Metagenomic analysis of the chemostat enrichment and reverse-transcription (RT) qPCR targeting *mbnA*

Shotgun metagenomic sequencing of the reactor culture was performed at Macrogen Inc. using a HiSeq X sequencing platform (Illumina) generating ~5 Gb of paired-end reads with 150-bp read length (accession number: SRX8210314). The raw short reads were quality-screened using Trimmomatic v0.36 with default parameters (65). The processed reads were assembled into contigs using metaSPAdes v3.12.0, and coding sequences were identified using Prodigal v2.6.3 (66, 67). The Hidden Markov model (HMM) algorithms for *nirS*, *nirK* and clade I and clade II *nosZ* were downloaded from the FunGene database (<http://fungene.cme.msu.edu/>). A previously constructed HMM algorithm for *mbnA* was used for screening of *mbnA* genes (68). The predicted contigs were screened for these targeted genes using *hmmsearch* in HMMER 3.1b2 with E-value set to 10^{-5} using these HMM algorithms. The identified gene sequences were further validated by running blastx

against the RefSeq database with E-value cut-off set to 10^{-3} . For taxonomy assignment, the translated amino acid sequences of the screened functional genes were searched against NCBI's non-redundant protein database (nr) using blastp with E-value cutoff of 10^{-10} . The quality-trimmed reads were mapped onto the screened functional gene sequences using the bowtie2 v2.3.4.1 software with the parameters set to default values (69). The coverage of each target gene was calculated using the *genomecov* command of the BEDtools v2.17.0 software and normalized by its length (70).

A degenerate primer set was designed with the sole unique *mbnA* sequence recovered from the shotgun metagenome data and publicly available *Methylocystis mbnA* sequences with >85% translated amino acid sequence identity with this metagenome-derived *mbnA* sequence (Supplementary Fig. S1) using Geneious v9.1.7 software (Biomatters Ltd., Auckland, New Zealand). This primer set (672f: 5'-GCTCGTCATACCATTCGGG-3' and 771r: 5'-GCTTGGCGATACGGATGGTC-3') was used for quantification of *mbnA* genes and transcripts in the chemostat culture (Supplementary Fig. S1).

Extraction and purification of RNA was performed using RNeasy Mini Kit (Qiagen) and RNA MinElute Kit (Qiagen), respectively, and reverse transcription was performed using SuperScript III reverse transcriptase (Invitrogen, Carlsbad, CA), according to the established protocols (71). As previously described, a known quantity of luciferase control mRNA (Promega, Madison, WI) was used as the internal standard to correct for RNA loss during extraction and purification procedure. The *mbnA* transcript copy numbers were normalized with *mbnA* copy numbers in the genomic DNA.

Statistical analyses

All experiments were performed in triplicates and the average values were presented with the error bars representing the standard deviations of triplicate samples. The statistical significance of the data from two different experimental conditions were tested with the two-sample *t*-tests, and statistical comparison between two different time points with one-sample *t*-tests. The SPSS statistics 24 software (IBM Corp, NY) was used for statistical analyses.

Acknowledgements

This work was supported by the National Research Foundation of Korea (Grants 2017R1D1A1B03028161 and 2015M3D3A1A01064881) and the United States Department of Energy (DE-SC0020174). The authors were also financially supported by the Brain Korea 21 Plus Project (Grant 21A20132000003).

Compliance with ethical standards

Conflict of interest

The authors declare that they have no conflict of interest.

Reference

1. Edenhofer O, Pichs-Madruga R, Sokona Y, Farahani E, Kadner S, Seyboth K, Adler A, Baum I, Brunner S, Eickemeier P. 2014. Climate Change 2014: Mitigation of Climate Change. Contribution of Working Group III to the Fifth Assessment Report of the Intergovernmental Panel on Climate Change. Cambridge University Press, Cambridge, United Kingdom.
2. Bridgman SD, Cadillo-Quiroz H, Keller JK, Zhuang Q. 2013. Methane emissions from wetlands: biogeochemical, microbial, and modeling perspectives from local to global scales. *Glob Change Biol* 19:1325-1346.
3. Yoon S, Song B, Phillips RL, Chang J, Song MJ. 2019. Ecological and physiological implications of nitrogen oxide reduction pathways on greenhouse gas emissions in agroecosystems. *FEMS Microbiol Ecol* 95:fiz066.
4. Jones CM, Spor A, Brennan FP, Breuil M-C, Bru D, Lemanceau P, Griffiths B, Hallin S, Philippot L. 2014. Recently identified microbial guild mediates soil N₂O sink capacity. *Nat Clim Change* 4:801-805.
5. Domeignoz-Horta LA, Spor A, Bru D, Breuil M-C, Bizouard F, Leonard J, Philippot L. 2015. The diversity of the N₂O reducers matters for the N₂O:N₂ denitrification end-product ratio across an annual and a perennial cropping system. *Front Microbiol* 6:971.
6. Ettwig KF, Zhu B, Speth D, Keltjens JT, Jetten MSM, Kartal B. 2016. Archaea catalyze iron-dependent anaerobic oxidation of methane. *Proc Natl Acad Sci* 113:12792-12796.
7. Ettwig KF, Butler MK, Le Paslier D, Pelletier E, Mangenot S, Kuypers MMM, Schreiber F, Dutilh BE, Zedelius J, de Beer D, Gloerich J, Wessels HJCT, van Alen T, Luesken F, Wu ML, van de Pas-Schoonen KT, Op den Camp HJM, Janssen-Megens EM, Francoijs K-J, Stunnenberg H, Weissenbach J, Jetten MSM, Strous M. 2010. Nitrite-driven anaerobic methane oxidation by oxygenic bacteria. *Nature* 464:543-548.
8. van Teeseling MCF, Pol A, Harhangi HR, van der Zwart S, Jetten MSM, Op den Camp HJM, van Niftrik L. 2014. Expanding the verrucomicrobial methanotrophic world: description of three novel species of *Methyloacidimicrobium* gen. nov. *Appl Environ Microbiol* 80: 6782-6791.
9. Dunfield PF, Yuryev A, Senin P, Smirnova AV, Stott MB, Hou S, Ly B, Saw JH, Zhou Z, Ren Y, Wang J, Mountain BW, Crowe MA, Weatherby TM, Bodelier PLE, Liesack W, Feng L, Wang L, Alam M. 2007. Methane oxidation by an extremely acidophilic bacterium of the phylum *Verrucomicrobia*. *Nature* 450:879-882.

10. Lee HJ, Jeong SE, Kim PJ, Madsen EL, Jeon CO. 2015. High resolution depth distribution of *Bacteria*, *Archaea*, methanotrophs, and methanogens in the bulk and rhizosphere soils of a flooded rice paddy. *Front Microbiol* 6:639.
11. Gebert J, Perner M. 2015. Impact of preferential methane flow through soil on microbial community composition. *Eur J Soil Biol* 69:8-16.
12. Semrau JD, DiSpirito AA, Yoon S. 2010. Methanotrophs and copper. *FEMS Microbiol Rev* 34: 496-531.
13. Lawton TJ, Rosenzweig AC. 2016. Biocatalysts for methane conversion: big progress on breaking a small substrate. *Curr Opin Chem Biol* 35:142-149.
14. Knief C. 2015. Diversity and habitat preferences of cultivated and uncultivated aerobic methanotrophic bacteria evaluated based on *pmoA* as molecular marker. *Front Microbiol* 6: 1346.
15. Choi DW, Kunz RC, Boyd ES, Semrau JD, Antholine WE, Han JI, Zahn JA, Boyd JM, Mora AM, DiSpirito AA. 2003. The membrane-associated methane monooxygenase (pMMO) and pMMO-NADH: quinone oxidoreductase complex from *Methylococcus capsulatus* Bath. *J Bacteriol* 185:5755-5764.
16. Semrau JD, DiSpirito AA, Gu W, Yoon S. 2018. Metals and methanotrophy. *Appl Environ Microbiol* 84:e02289-17.
17. Balasubramanian R, Smith SM, Rawat S, Yatsunyk LA, Stemmler TL, Rosenzweig AC. 2010. Oxidation of methane by a biological dicopper centre. *Nature* 465:115-119.
18. DiSpirito AA, Semrau JD, Murrell JC, Gallagher WH, Dennison C, Vuilleumier S. 2016. Methanobactin and the link between copper and bacterial methane oxidation. *Microbiol Mol Biol Rev* 80: 387-409.
19. Gu W, Ul Haque MF, Baral BS, Turpin EA, Bandow NL, Kremmer E, latley A, Zischka H, DiSpirito AA, Semrau JD. 2016. A TonB-dependent transporter is responsible for methanobactin uptake by *Methylosinus trichosporium* OB3b. *Appl Environ Microbiol*. 82: 1917-1923.
20. Dassama LMK, Kenney GE, Ro SY, Zielazinski EL, Rosenzweig AC. . 2016. Methanobactin transport machinery. *Proc Nat Acad Sci* 113:13027-13032.
21. Bandow N, Gilles VS, Freesmeier B, Semrau JD, Krentz B, Gallagher W, McEllistrem MT, Hartsel SC, Choi DW, Hargrove MS, Heard TM, Chesner LN, Braunreiter KM, Cao BV, Gavitt MM, Hoopes JZ, Johnson JM, Polster EM, Schoenick BD, Umlauf AM, DiSpirito AA. 2012. Spectral and copper binding properties of methanobactin from the facultative methanotroph *Methylocystis* strain SB2. *J Inorg Biochem* 110:72-82.
22. Kim HJ, Graham DW, DiSpirito AA, Alterman MA, Galeva N, Larive CK, Asunskis D, Sherwood PMA. 2004. Methanobactin, a copper-acquisition compound from methane-oxidizing bacteria. *Science* 305: 1612-1615.
23. El Ghazouani A, Baslé A, Gray J, Graham DW, Firbank SJ, Dennison C. 2012. Variations in methanobactin structure influences copper utilization by methane-oxidizing bacteria. *Proc Nat Acad Sci* 109:8400-8404.
24. Kenney GE, Goering AW, Ross MO, DeHart CJ, Thomas PM, Hoffman BM, Kelleher NL. 2016. Characterization of Methanobactin from *Methylosinus* sp. LW4. *J Am Chem Soc* 138:11124-11127.
25. Godden JW, Turley S, Teller DC, Adman ET, Liu MY, Payne WJ, LeGall J. 1991. The 2.3 angstrom X-ray structure of nitrite reductase from *Achromobacter cycloclastes*. *Science* 253:438-442.
26. Brown K, Tegoni M, Prudêncio M, Pereira AS, Besson S, Moura JJ, Moura I, Cambillau C. 2000. A novel type of catalytic copper cluster in nitrous oxide reductase. *Nat Struct Biol* 7:191-195.
27. Lawton TJ, Ham J, Sun T, Rosenzweig AC. 2014. Structural conservation of the B subunit in the ammonia monooxygenase/particulate methane monooxygenase superfamily. *Proteins* 82: 2263-2267.
28. Thomson AJ, Giannopoulos G, Pretty J, Baggs EM, Richardson DJ. 2012. Biological sources and sinks of nitrous oxide and strategies to mitigate emissions. *Philos Trans R Soc B* 367:1157–1168.

29. Gwak JH, Jung MY, Hong H, Kim JG, Quan ZX, Reinfelder JR, Spasov E, Neufeld JD, Wagner M, Rhee S-K. 2019. Archaeal nitrification is constrained by copper complexation with organic matter in municipal wastewater treatment plants. *ISME J* 14:335-346.
30. Chang J, Gu W, Park D, Semrau JD, DiSpirito AA, Yoon S. 2018. Methanobactin from *Methylosinus trichosporium* OB3b inhibits N₂O reduction in denitrifiers. *ISME J* 12:2086-2089.
31. Lee A, Winther M, Priemé A, Blunier T, Christensen S. 2017. Hot spots of N₂O emission move with the seasonally mobile oxic-anoxic interface in drained organic soils. *Soil Biol Biochem* 115:178-186.
32. Bush T, Diao M, Allen RJ, Sinnige R, Muyzer G, Huisman J. 2017. Oxic-anoxic regime shifts mediated by feedbacks between biogeochemical processes and microbial community dynamics. *Nat Commun* 8:1-9.
33. Sullivan MJ, Gates AJ, Appia-Ayme C, Rowley G, Richardson DJ. 2013. Copper control of bacterial nitrous oxide emission and its impact on vitamin B₁₂-dependent metabolism. *Proc Natl Acad Sci* 110:19926-19931.
34. Twining BS, Mylon SE, Benoit G. 2007. Potential role of copper availability in nitrous oxide accumulation in a temperate lake. *Limnol Oceanogr* 52:1354-1366.
35. Granger J, Ward BB. 2003. Accumulation of nitrogen oxides in copper-limited cultures of denitrifying bacteria. *Limnol Oceanogr* 48:313-318.
36. Zumft WG. 1997. Cell biology and molecular basis of denitrification. *Microbiol Mol Biol Rev* 61:533-616.
37. Bannert A, Kleineidam K, Wissing L, Mueller-Niggemann C, Vogelsang V, Welzl G, Cao Z, Schloter M. 2011. Changes in diversity and functional gene abundances of microbial communities involved in nitrogen fixation, nitrification, and denitrification in a tidal wetland versus paddy soils cultivated for different time periods. *Appl Environ Microbiol* 77: 6109-6116.
38. Dam B, Dam S, Blom J, Liesack W. 2013. Genome analysis coupled with physiological studies reveals a diverse nitrogen metabolism in *Methylocystis* sp. strain SC2. *PLoS ONE* 8:e74767.
39. Stein LY, Bringel F, DiSpirito AA, Han S, Jetten MSM, Kalyuzhnaya MG, Kits KD, Klotz MG, Op den Camp HJM, Semrau JD, Vuilleumier S, Bruce DC, Cheng J-F, Davenport KW, Goodwin L, Han S, Hauser L, Lajus A, Land ML, Lapidus A, Lucas S, Médigue C, Pitluck S, Woyke T. 2011. Genome sequence of the methanotrophic Alphaproteobacterium *Methylocystis* sp. strain Rockwell (ATCC 49242). *J Bacteriol* 193:2668-2669.
40. Roco CA, Bergaust LL, Bakken LR, Yavitt JB, Shapleigh JP. 2017. Modularity of nitrogen-oxide reducing soil bacteria: linking phenotype to genotype. *Environ Microbiol* 19:2507-2519.
41. Lycus P, Bøthun KL, Bergaust L, Shapleigh JP, Bakken LR, Frostegård Å. 2017. Phenotypic and genotypic richness of denitrifiers revealed by a novel isolation strategy. *ISME J* 11:2219-2232.
42. Choi DW, Do YS, Zea CJ, McEllistrem MT, Lee SW, Semrau JD, Pohl NL, Kisting CJ, Scardino LL, Hartsel SC, Boyd ES, Geesey GG, Riedel TP, Shafe PH, Kranski KA, Tritsch JR, Antholine WE, DiSpirito AA. 2006. Spectral and thermodynamic properties of Ag (I), Au (III), Cd (II), Co (II), Fe (III), Hg (II), Mn (II), Ni (II), Pb (II), U (IV), and Zn (II) binding by methanobactin from *Methylosinus trichosporium* OB3b. *J Inorg Biochem* 100:2150-2161.
43. Yoon S, Kraemer SM, DiSpirito AA, Semrau JD. 2010 An assay for screening microbial cultures for chalkophore production. *Environ Microbiol Rep* 2:295-303.
44. Karlsen OA, Berven FS, Stafford GP, Larsen Ø, Murrell JC, Jensen HB, Fjellbirkeland A. 2003. The surface-associated and secreted MopE protein of *Methylococcus capsulatus* (Bath) responds to changes in the concentration of copper in the growth medium. *Appl Environ Microbiol* 69:2386-2388.
45. Johnson KA, Ve T, Larsen Ø, Pedersen RB, Lillehaug JR, Jensen HB, Helland R, Karlsen OA. 2014. CorA is a copper repressible surface-associated copper (I)-binding protein produced in *Methylomicrobium album* BG8. *PLoS ONE* 9:e87750.
46. Prosser JI. 2015. Dispersing misconceptions and identifying opportunities for the use of 'omics' in soil microbial ecology. *Nat Rev Microbiol* 13:439-446.
47. Baveye PC, Otten W, Kravchenko A, Balseiro-Romero M, Beckers É, Chalhoub M, Darnault C, Eickhorst T, Garnier P, Hapca S, Kiranyaz S, Monga O, Mueller CW, Nunan N, Pot V, Schlüter S, Schmidt H, Vogel H-J. 2018. Emergent properties of microbial activity in heterogeneous soil

- microenvironments: different research approaches are slowly converging, yet major challenges remain. *Front Microbiol* 9:1929.
48. Alam MS, Jia Z. 2012. Inhibition of methane oxidation by nitrogenous fertilizers in a paddy soil. *Front Microbiol*. 3:246.
 49. Reim A, Lüke C, Krause S, Pratscher J, Frenzel P. 2012. One millimetre makes the difference: high-resolution analysis of methane-oxidizing bacteria and their specific activity at the oxic-anoxic interface in a flooded paddy soil. *ISME J* 6:2128-2139.
 50. Ma K, Conrad R, Lu Y. Dry/wet cycles change the activity and population dynamics of methanotrophs in rice field soil. *Appl Environ Microbiol* 2013 79:4932-4939.
 51. Davidson EA, Verchot LV, Cattânio JH, Ackerman IL, Carvalho JEM. 2000. Effects of soil water content on soil respiration in forests and cattle pastures of eastern Amazonia. *Biogeochemistry*. 48:53-69.
 52. Sastre J, Sahuquillo A, Vidal M, Rauret G. 2002. Determination of Cd, Cu, Pb and Zn in environmental samples: microwave-assisted total digestion versus aqua regia and nitric acid extraction. *Anal Chim Acta* 462:59-72.
 53. Whittenbury R, Phillips KC, Wilkinson JF. 1970. Enrichment, isolation and some properties of methane-utilizing bacteria. *Microbiology* 61:205-218.
 54. Wolin EA, Wolfe RS, Wolin MJ. 1964. Viologen dye inhibition of methane formation by *Methanobacillus omelianskii*. *J Bacteriol* 87:993-998.
 55. Yoon S, Sanford RA, Löffler FE. 2015. Nitrite control over dissimilatory nitrate/nitrite reduction pathways in *Shewanella loihica* strain PV-4. *Appl Environ Microbiol* 81:3510-3517.
 56. Sander R. 2015. Compilation of Henry's law constants (version 4.0) for water as solvent. *Atmos Chem Phys* 15:4399-4981.
 57. Miranda KM, Espey MG, Wink DA. 2001. A rapid, simple spectrophotometric method for simultaneous detection of nitrate and nitrite. *Nitric Oxide* 5:62-71.
 58. Baethgen WE, Alley MM. 1989. A manual colorimetric procedure for measuring ammonium nitrogen in soil and plant Kjeldahl digests. *Commun Soil Sci Plant Anal* 20:961-969.
 59. Ritalahti KM, Amos BK, Sung Y, Wu Q, Koenigsberg SS, Löffler FE. 2006. Quantitative PCR targeting 16S rRNA and reductive dehalogenase genes simultaneously monitors multiple *Dehalococcoides* strains. *Appl Environ Microbiol*. 72: 2765-74.
 60. Bandow NL, Gallagher WH, Behling L, Choi DW, Semrau JD, Hartsel SC, Gilles VS, DiSpirito AA. 2011. Isolation of methanobactin from the spent media of methane-oxidizing bacteria. *Methods Enzymol* 495:259-269.
 61. Kim J, Kim DD, Yoon S. 2018. Rapid isolation of fast-growing methanotrophs from environmental samples using continuous cultivation with gradually increased dilution rates. *Appl Microbiol Biotechnol* 102:5707-5715.
 62. Gu W, Baral BS, DiSpirito AA, Semrau JD. 2017. An aminotransferase is responsible for the deamination of the N-terminal leucine and required for formation of oxazolone ring A in methanobactin of *Methylosinus trichosporium* OB3b. *Appl Environ Microbiol* 83:e02619-16.
 63. Matsuki T, Watanabe K, Fujimoto J, Miyamoto Y, Takada T, Matsumoto K, Oyaizu H, Tanaka R. 2002. Development of 16S rRNA-gene-targeted group-specific primers for the detection and identification of predominant bacteria in human feces. *Appl Environ Microbiol* 68:5445-5451.
 64. Caporaso JG, Kuczynski J, Stombaugh J, Bittinger K, Bushman FD, Costello EK, Fierer N, Pena AG, Goodrich JK, Gordon JI, Huttley GA, Kelley ST, Knights D, Koenig JE, Ley RE, Lozupone CA, McDonald D, Muegge BD, Pirrung M, Reeder J, Sevinsky JR, Turnbaugh PJ, Walters WA, Widmann J, Yatsunenko T, Zaneveld J, Knight R. 2010. QIIME allows analysis of high-throughput community sequencing data. *Nat Methods* 7:335-336.
 65. Bolger AM, Lohse M, Usadel B. 2014. Trimmomatic: a flexible trimmer for Illumina sequence data. *Bioinformatics* 30:2114-2120.
 66. Hyatt D, Chen GL, LoCascio PF, Land ML, Larimer FW, Hauser LJ. 2010 Prodigal: prokaryotic gene recognition and translation initiation site identification. *BMC Bioinform* 11:119.
 67. Nurk S, Meleshko D, Korobeynikov A, Pevzner PA. 2017. metaSPAdes: a new versatile metagenomic assembler. *Genome Res* 27:824-834.

68. Kenney GE, Rosenzweig AC. 2013. Genome mining for methanobactins. *BMC Biol* 11:17.
69. Langmead B, Salzberg SL. 2012. Fast gapped-read alignment with Bowtie 2. *Nat Methods* 9:357-359.
70. Quinlan AR. 2014. BEDTools: the Swiss-army tool for genome feature analysis. *Curr Protoc Bioinform* 47:11.12.1-34.
71. Yoon S, Cruz-García C, Sanford R, Ritalahti KM, Löffler FE. 2015. Denitrification versus respiratory ammonification: environmental controls of two competing dissimilatory $\text{NO}_3^-/\text{NO}_2^-$ reduction pathways in *Shewanella loihica* strain PV-4. *ISME J* 9:1093-1104.

Figures

FIG 1

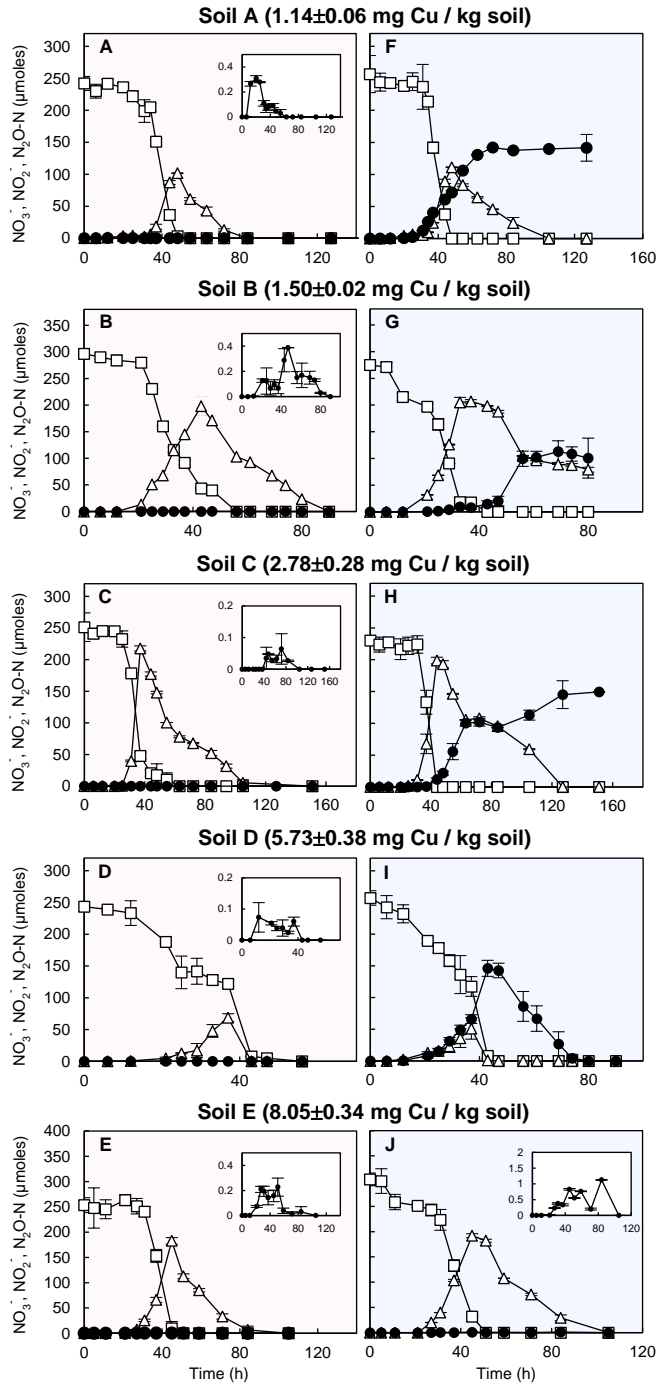


FIG 1 Denitrification of 250 μmoles (5 mM) NO₃⁻ added to 50 mL rice paddy soil suspensions in 160-mL serum bottles amended without (A-E; shaded red) and with (F-J; shaded blue) 10 μM OB3b-MB. The copper content of the rice paddy soils used for preparation of the suspensions were 1.14 (A,

F), 1.50 (B, G), 2.78 (C, H), 5.73 (D, I), and 8.05 (E, J) mg Cu / kg dry wt. The time series of the average amounts (μ moles per vessel) of NO_3^- (\square), NO_2^- (Δ), and N_2O (\bullet) are presented with the error bars representing the standard deviations of triplicate samples. The inserts are magnification of the N_2O monitoring data.

FIG 2

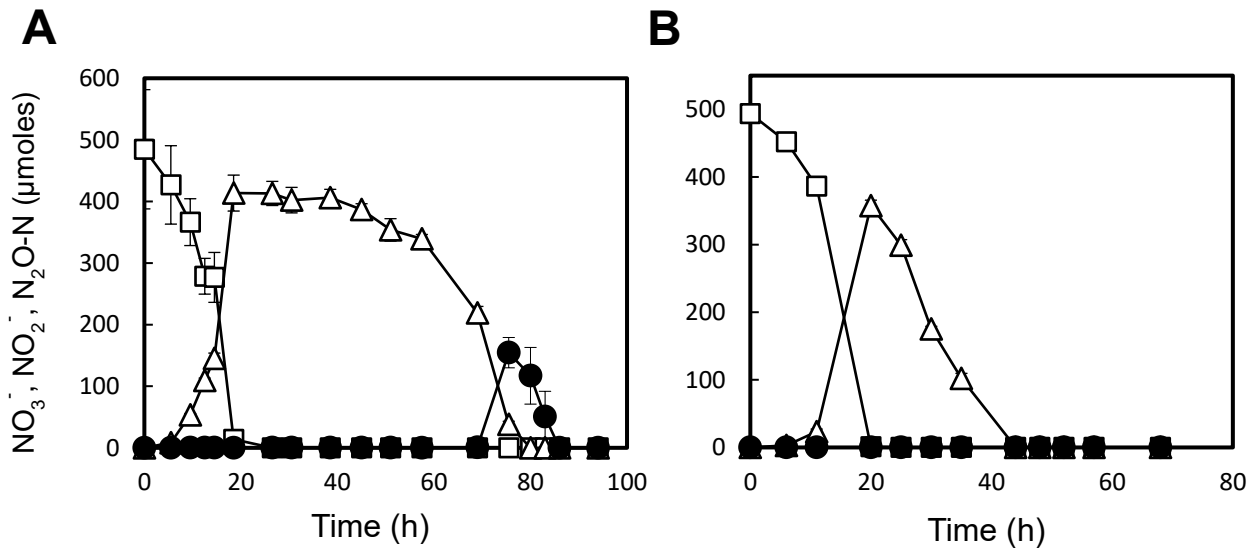


FIG 2 (A) Progression of denitrification in the 50-mL enrichment cultures (in 160-mL serum bottles with N_2 headspace) extracted from the *Methylocystaceae*-dominant chemostat. One milliliter of separately prepared denitrifier enrichment culture was added to the enrichment cultures at $t=0$. To a set of controls (B), CuCl_2 was added to a concentration of $2 \mu\text{M}$ before incubation. The changes to the amounts of NO_3^- (\square), NO_2^- (Δ), and N_2O (\bullet) in the culture vessels were monitored. The error bars represent the standard deviations of triplicate samples.

FIG 3

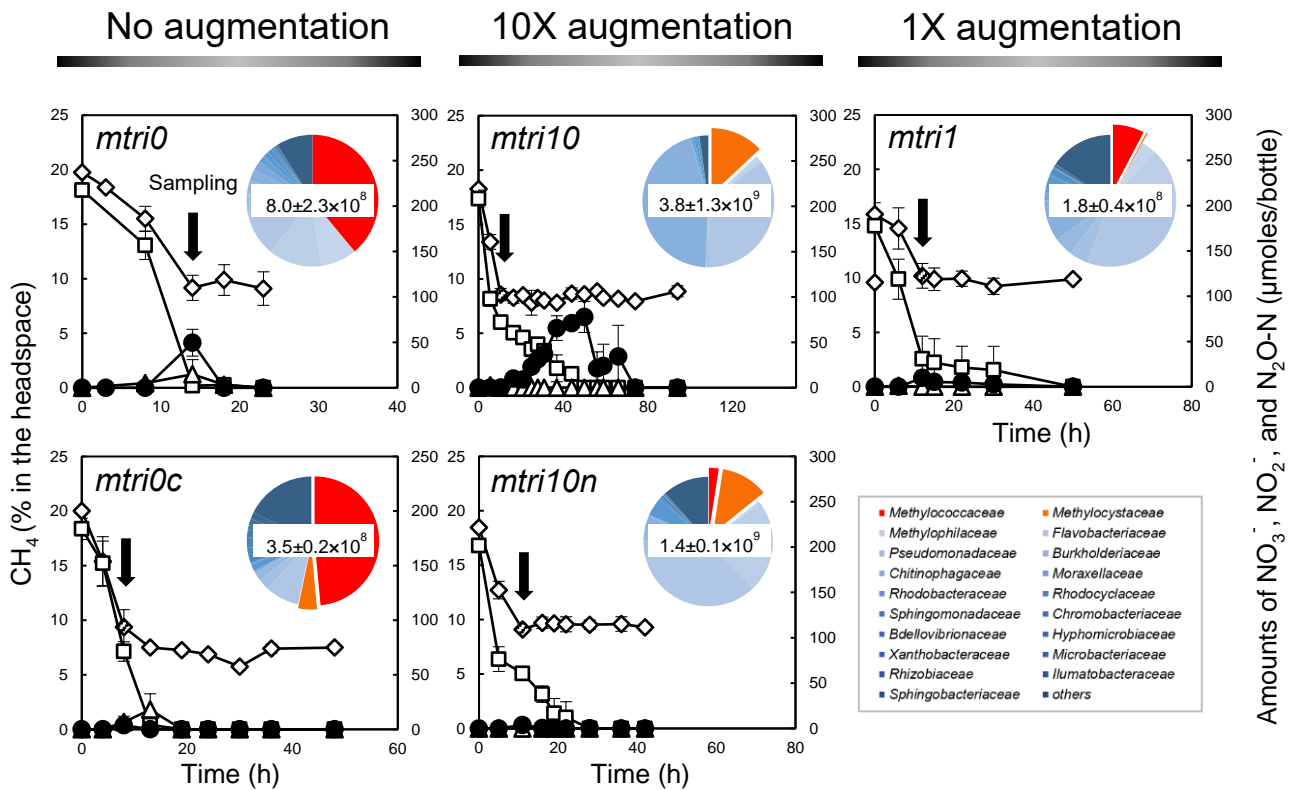


FIG 3 Monitoring of CH₄ oxidation and subsequent denitrification and N₂O production in rice paddy soil suspensions augmented with *M. trichosporium* OB3b (or $\Delta mbnAN$ mutant) cells prior to incubation to quantities with their *pmoA* copy numbers matching 0 (*mtri0*, *mtri0c*), 1 (*mtri1*), and 10 (*mtri10*, *mtri10n*) times the estimated *Methylococcaceae* 16S rRNA gene copy numbers in the suspensions. The Cu-replete control, to which 2 μ M CuCl₂ was added (*mtri1c*), and the control augmented with $\Delta mbnAN$ mutant of *M. trichosporium* (*mtri10n*) were included. The time series of the amounts (μ moles per vessel) of NO₃⁻ (□), NO₂⁻ (Δ), and N₂O (●) and the headspace concentrations (%) of CH₄ (◇) are presented with the error bars representing the standard deviations of triplicate samples. The pie charts embedded in the panels illustrate the microbial community compositions of the enrichment cultures at the time points indicated by the black arrows. The numbers in the center of the pie charts are the estimates of bacterial 16S rRNA copy numbers per mL of culture at the indicated time points. The detailed microbial community compositions are presented in Supplementary Table S4.

1 **Table**2 **Table 1.** List of the primers/probe sets used for qPCR and RT-qPCR analyses

3

Primer set	Target gene	Amplicon length (bp)	Slope	y-intercept	Amplification efficiency	R ²	Reference
16S rRNA 1055f: 5'-ATGGCTGTCGTCAGCT-3'	Bacterial 16S rRNA	338	-3.30	37.7	101.1	0.996	(59)
16S rRNA 1392r: 5'-ACGGGCGGTGTGTAC-3'							
Bac1115_probe: 5'-CAACGAGCGCAACCC-3'							
OB3b_pmoAf: 5'-CGCTCGACATGCGGATAT-3'	<i>pmoA</i>	266	-3.38	36.4	97.8	0.998	This study
OB3b_pmoAr: 5'-TTTCCCGATCAGCCTGGT-3'							
OB3b_pmoA_probe: 5'-AGCCACAGCGCCGGAACCA-3'							
mbnAf672: 5'-GCTCGTCATACCATTCGGG-3'	<i>mbnA</i>	100	-3.32	37.7	100.1	0.999	This study
mbnAr771: 5'-GCTTGGCGATACGGATGGTC-3'							
lucf: 5'-TACAACACCCCAACATCTTCGA-3'	luciferase control mRNA	67	-3.37	37.1	98.0	0.999	(71)
lucr: 5'-GGAAGTTCACCGGCGTCAT-3'							

4